Adiabatic and nonadiabatic energy dissipation during scattering of vibrationally excited CO from Au(111)

Meng Huang, Xueyao Zhou, Yaolong Zhang, Linsen Zhou, Maite Alducin, Bin Jiang, and Hua Guo

Phys. Rev. B **100**, 201407 — Published 25 November 2019

DOI: 10.1103/PhysRevB.100.201407

Adiabatic and Nonadiabatic Energy Dissipation during Scattering of Vibrationally Excited CO from Au(111)

Meng Huang,[1] Xueyao Zhou,[1,2] Yaolong Zhang,[2] Linsen Zhou,[1] Maite Alducin,[3,4] Bin Jiang,[2] and Hua Guo[1,*]

[1]*Department of Chemistry and Chemical Biology, University of New Mexico, Albuquerque, New Mexico 87131, USA*
[2]*Department of Chemical Physics, University of Science and Technology of China, Hefei, Anhui 230026, China*
[3]*Centro de Física de Materiales, CSIC-UPV/EHU, P. Manuel de Lardizabal 5, 20018 San Sebastián, Spain*
[4]*Donostia International Physics Center DIPC, P. Manuel de Lardizabal 4, 20018 San Sebastián, Spain*

A high-dimensional potential energy surface (PES) for CO interaction with the Au(111) surface is developed using a machine-learning algorithm. Including both molecular and surface coordinates, this PES enables the simulations of the recent experiment on scattering of vibrationally excited CO from Au(111). Trapping in a physisorption well is observed to increase with decreasing incidence energy. While energy dissipation of physisorbed CO is slow, due to weak coupling with both the phonons and electron-hole pairs, the access of the impinging CO to the chemisorption well facilitates its fast vibrational relaxation through nonadiabatic coupling with surface electron-hole pairs. The latter is proposed as a mechanism for the experimentally observed fast component of CO(v=1) product that has remained unexplained so far.

Energy transfer between molecules and metal surfaces represents a key aspect of surface processes, with important implications in a wide array of interfacial phenomena. There are two major energy exchange channels, namely the adiabatic coupling with surface phonons and the nonadiabatic interaction with electron-hole pairs (EHPs).[1-4] The lifetime of CO(v=1) adsorbate has been measured to be 1-2 ps on Cu(100), using several experimental techniques.[5-8] Such a short lifetime for a high frequency mode (ω=2129 cm^{-1}) can only be explained by its nonadiabatic coupling with surface EHPs, because its direct coupling with the low-frequency phonons requires many such quanta. This nonadiabatic energy dissipation mechanism has been characterized by various theoretical models,[9-19] cumulating with the latest first-principles calculations that quantitatively reproduced the observed lifetime.[20,21]

It was thus a surprise when Shirhatti et al. reported recently a long estimated lifetime (~10^2 ps) for trapped CO(v=1) in the scattering of vibrationally excited CO(v=2) from Au(111).[22] It was postulated that physisorption might be involved, given the relatively low desorption temperature of CO from Au(111).[23] Indeed, a recent density functional theory (DFT) study by Lonc□arić et al. did find such a physisorption well for CO on Au(111),[24] using the Bayesian Error Estimation Functional method with van der Waals corrections (BEEF-vdW).[25] The lifetime of physisorbed CO(v=1) was calculated within first-principles many-body perturbation theory and found to be consistent with the experimental estimate.[24] The long vibrational lifetime was attributed to the weak couplings with EHPs because of the large distance between the adsorbate and surface. The same argument has also been used to explain the vibrationally hot precursor CH_4 on the Ir(111) surface.[26] Very recently, the CO(v=1) lifetime on Au(111) was measured directly to be 49±3 ps, confirming the physisorption nature of this system.[27]

In addition to the long-lived CO, a fast component was also observed in the desorbed CO(v=1),[22] which has so far defied an explanation. Although Ab Initio Molecular Dynamics (AIMD) can shed light on such an issue, the trapping and diffusion are too rare and too long to be computationally feasible for the on-the-fly method. To meet this challenge, we report here a machine-learning approach which trains neural networks (NNs) to predict the high-dimensional potential energy surface (PES) for the CO/Au(111) system, thus avoiding the expensive on-the-fly DFT calculations in AIMD. Based on the original idea of Behler and Parrinello,[28,29] atomistic NNs (AtNN) can be designed to include both the molecular and surface degrees of freedom (DOFs) within a periodic slab model,[30-33] thus allowing adiabatic energy exchange between the impinging molecule and surface phonons. To this end, a 60-dimensional PES is trained using both energies and gradients from AIMD calculations, which enables large numbers of quasi-classical trajectories (QCTs) to determine trapping probabilities and to follow the long-time diffusion dynamics of the trapped species. In addition, a generalized Langevin equation (GLE) with electronic friction (EF) coefficients,[34] denoted as QCTEF, is used to simulate the nonadiabatic energy dissipation of the CO adsorbate to surface EHPs.[2] A combination of these theoretical advances allows a detailed characterization of the trapping and energy dissipation during the scattering, thus shedding valuable light on the intricate interplay between adiabatic and nonadiabatic energy exchanges.

To generate the initial data points for building the PES, AIMD simulations of CO scattering from Au(111) were

first performed using the Vienna Ab Initio Simulation Package (VASP) [35,36] with the BEEF-vdW functional.[25] In these simulations, Au(111) was approximated by a slab with 4 layers of a 3×3 unit cell with the bottom two layers frozen, which is separated from its images by 16 Å of vacuum. The cut-off energy in the planewave basis was 450 eV and the Brillouin zone sampled with a 5×5×1 Monkhorst-Pack mesh. The slab was thermalized to 300K and the geometries and velocities of the surface atoms were randomly sampled. The CO(v=2, J=0) molecule, with its internal coordinate and momentum sampled on the gas phase CO potential, was prepared from 8 Å above the surface with random orientations and positions in the unit cell. Following the experiment,[22] the incidence angle was fixed at θ=9° from the surface normal. A total of 100 and 80 trajectories was calculated respectively at the experimental incidence energies of 0.64 and 1.28 eV.[22] Since these AIMD simulations are mainly for sampling the PES, they were performed with a timestep of 2.0 fs and the maximum value of total simulation time is 1 ps.

In the Behler−Parrinello approach,[28] the total energy of the system is obtained by summing atomic energies, which are represented by AtNNs for different atomic types. The environment of an atom is described by mapping (or symmetry) functions, which contain two- and three-body interactions.[29,37] The NN was trained by 10766 DFT points with the root mean square errors in the energy of entire cell and atomic force of 9.78 meV and 20.00 meV/Å. More details of the fitting are given in Supplemental Material (SM)[38] and Ref. [39].

Similar to the previous theoretical work,[24] there is a physisorption well with a depth of ~0.10 eV and a large distance from the surface (Z~4.0 Å). The parallelly oriented CO has a slightly deeper well than the perpendicularly oriented CO. In addition, a chemisorption well with 0.13 eV in depth is found at the top site, while it becomes metastable at the hollow site. These chemisorption wells feature a perpendicularly oriented CO with a shorter C-O bond and are much closer to the surface (Z~2.9 Å). A barrier of 61 meV exists from the physisorption well. The adsorption energies in various wells are smaller than the experimental estimation (0.18±0.10 eV).[23] To better simulate the experiment, the AtNN PES is modified to have a desorption energy of 0.18 eV, by adding a simple correcting potential as a function of the CO distance from the surface (details given in SM[38]).

In Fig. 1, two-dimensional cuts of the modified AtNN PES at two surface sites are displayed as functions of the CO bond length (r) and distance from the CO center of mass (COM) to surface (Z), with CO oriented either parallel and perpendicular to the surface normal, and the surface atoms were kept frozen at their equilibrium positions. These plots illustrate the topological features of the PES discussed above.

To explore the scattering dynamics, a total of 15,000 QCT trajectories was launched towards the surface at a surface temperature T_s=300K with the incident kinetic energy E_{in} set at the experimental values, 0.64, 0.40 and 0.32 eV. The initial conditions are identical to the AIMD calculations, but the propagation time is extended to 50 ps. These extensive QCT simulations were made possible by a ~10^5 acceleration over the on-the-fly AIMD. More details of QCT calculations can be found in SM,[38] and Refs. [40-44]

The QCT simulation results on the modified PES are presented below, but those on the original PES are given in SM.[38] While the majority of the trajectories undergo scattering back to the vacuum, there is a small portion that never desorbs at the end of the 50 ps run, which are denoted as "trapped" (T). The scattered trajectories are further divided into two categories; the ones with a single inner turning point are classified as "direct scattered" (DS), while those with multiple inner turning points are called "trapped then scattered" (TS). The fractions of these three types of trajectories are given in Table S1 in SM,[38] along with the averaged translational (<E_{trans}>), rotational (<E_{rot}>), and

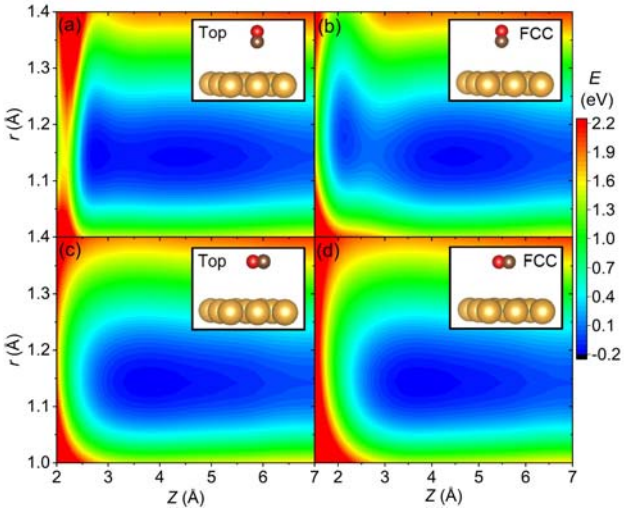

FIG. 1 Two-dimensional PES cuts at the top (a,c) and fcc (b,d) sites with different CO orientations.

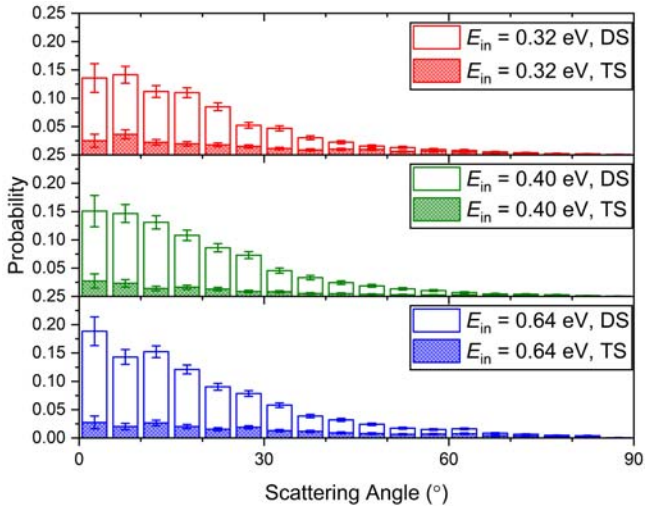

FIG. 2 Angular distributions of the scattered CO for DS (open) and TS (shaded) trajectories at three incidence energies.

vibrational (<$E_{vib,f}$>) energies. The probability of the trapped trajectories is 4.5% at 0.64 eV, but increases to 24% at 0.32 eV. This agrees with the observed experimental trend that significantly long-lived CO molecules were found at low incidence energies.[22]

The angular distributions of the scattered CO are displayed in **Error! Reference source not found.**. As expected, the dominant DS trajectories are mostly specular, with the distribution mostly centered around 10°, in good agreement with the experimental value of ~9°.[22] On the other hand, TS trajectories have a much broader angular distribution, also consistent with the experiment.[22] As shown in Table S1, the collision of CO with the surface results in energy redistribution among different DOFs. Figure 3 displays ratios between the final and initial energies in different DOFs. As seen in Fig. 3(a), the total energy of CO decreases about 20% after scattering, apparently lost to surface DOFs. Among the molecular DOFs, the vibrational energy ratio (Fig. 3(b)) ranges from 0.92 to 1.08, suggesting strong vibrational elasticity, consistent with the large frequency mismatch between CO vibration and surface phonons. On the other hand, significant energy is transferred to CO rotation, as shown in Fig. 3(c). Figure 3(d) indicates that the energy loss in the translational DOF is quite substantial. Beyond the limit of E_{trans}/E_{in}=0 is the trapping of CO, in which the molecule has insufficient kinetic energy to escape the adsorption well. These trapped CO adsorbates experience facile diffusion along the surface, accompanied by nearly free rotation.

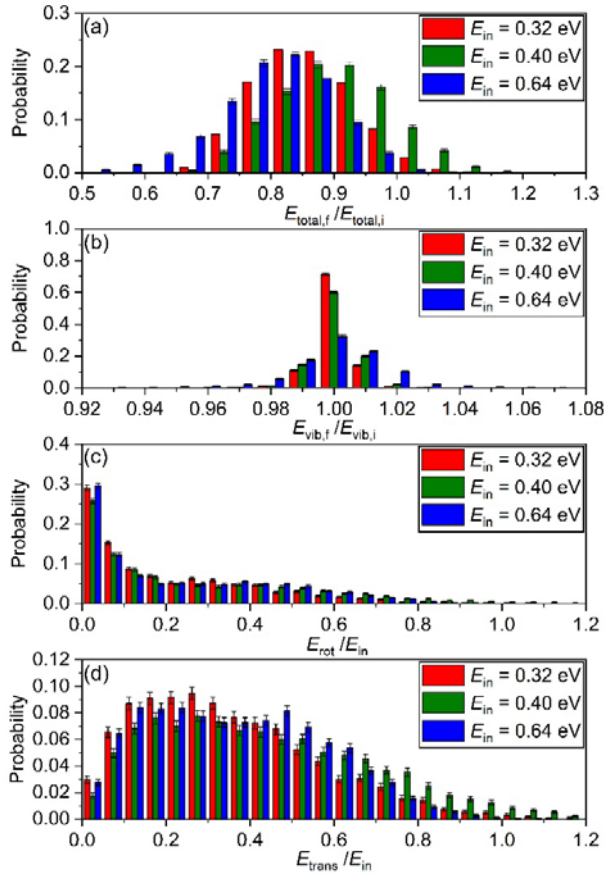

FIG. 3 Distributions of the total energy ratio ($E_{total,f}/E_{total,i}$), vibrational energy ratio ($E_{vib,f}/E_{vib,i}$), relative rotational energy ratio (E_{rot}/E_{in}), relative translational energy ratio (E_{trans}/E_{in}) for scattered CO at three different incidence energies E_{in}.

Trapping probabilities for the three incident energies are shown in Fig. 4(a) to decay exponentially and the lifetimes have been estimated. The lifetime (τ_0) of trapped CO on the surface, extracted from the slope in the logarithmic plot, are 99.2, 161.3, and 229.9 ps for E_{in} = 0.64, 0.40, and 0.32 eV, respectively. These lifetimes are similar to those reported in the experiment (~100 ps)[22] as well as static theoretical calculations.[24] These values are substantially larger than the CO lifetimes calculated with the unmodified PES, as shown in SM,[38] underscoring the dependence on the depth of the physisorption well. Finally, we note in passing that the system is unlikely to have reached thermal equilibrium as the lifetime in the figure changes with the

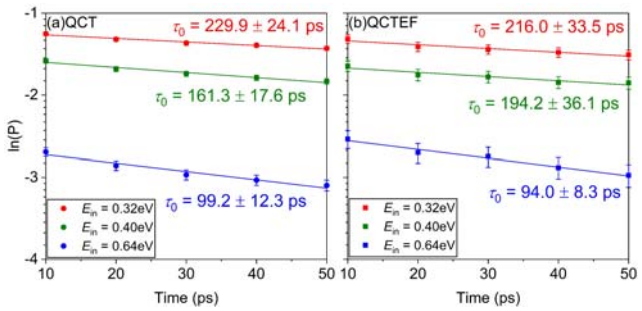

FIG. 4 Fraction of the CO molecules on the surface (Z<8.0Å) as a function of time for (a) QCT trajectories within the adiabatic approximation and (b) QCTEF trajectories with electronic friction.

incident energy.

To examine the role of EHPs, we investigated the nonadiabatic energy dissipation using the QCTEF approach. In particular, the atomic friction coefficients of CO were obtained within the local density friction approximation (LDFA),[45] in which CO is assumed to move in a free-electron gas at the metal surface. The surface electron density was approximated from DFT calculations of perfect Au(111), which is expected to be a reasonable approximation even for the moving surface.[46] The friction coefficients of the C and O atoms in the electron gas, which are proportional to the transport cross-section at the Fermi level,[47] can be calculated with the position of the atom and the corresponding electron density (see SM[38] for more details). The QCTEF dynamics were carried out with the same initial conditions. The

nonadiabatic trapping probabilities shown in Fig. 4(b) are essentially the same as the adiabatic results within the error bars. Other dynamic attributes shown in SM[38] are also similar. This can be readily understood as the electron density in the physisorption well is vanishingly small, resulting in negligible friction coefficients. The weak EHP coupling is consistent with the long lifetime reported in the recent experiments[22,27] and first-principles calculations of the vibrational relaxation of CO physisorbed on Au(111).[24]

A puzzling and yet unexplained experimental observation is that the desorbed CO(v=1) product has both fast and slow components.[22] As discussed above, our adiabatic simulations produce little vibrational relaxation and the only possible mechanism is due to EHPs. Yet, our QCTEF results above also indicate that this nonadiabatic mechanism is unlikely if the CO is in the physisorption well, confirming the earlier static study.[24] Interestingly, a few impinging CO were found in our calculations to explore the chemisorption well and get trapped near the hollow site, thanks to the barrier between the physisorption and chemisorption wells shown in Fig. 1. However, such trapping trajectories are not common, due apparently to the entropically unfavorable requirement that CO needs to have an orientation perpendicular to the surface with the C-end down. Once trapped in the chemisorption well, however, QCTEF calculations indicated that CO undergoes a rapid loss of energy, due to the much larger friction coefficients stemming from much higher electron density near the surface at the hollow site. In Fig. 5, the energy loss of such an exemplary trajectory is shown, along with the time evolution of the Z and r coordinates. In this particular case, the impinging CO has a direct hit at the chemisorption well,

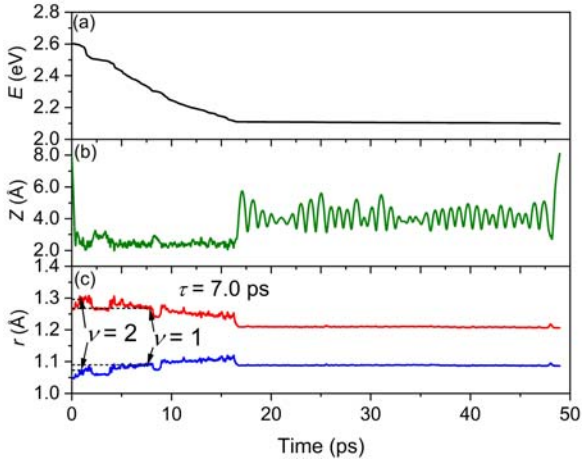

FIG. 5 Evolution of (a) total energy of the cell (b) CO COM distance from surface (Z) (c) CO bond length (r) at the outer (red) and inner (blue) vibrational turning points of an exemplary trajectory at E_{in} = 0.32 eV.

followed by transient trapping in the well before escaping to the physisorption well and finally desorbing. However, this is not always the case in other trajectories, which may first get trapped in the physisorption well before entering the chemisorption well. It is clear from the figure that the rapid EHP-induced energy dissipation occurring in the chemisorption well leads to significant energy loss in the vibrational DOF, as evidenced by the changes of the vibrational turning points in the figure. It is thus likely that the experimentally observed CO(v=1) stems from initial access of the chemisorption well, where rapid vibrational relaxation takes place. The rapid desorption of such relaxed CO molecules leads to the experimentally observed fast component of the velocity distribution of desorbed CO(v=1), while those trapped in the physisorption well give rise to the slow component.

To conclude, a high-dimensional PES developed with a machine-learning algorithm allows detailed simulations of CO scattering dynamics from Au(111). Calculated attributes of the scattered trajectories, such as the angular distributions, are in excellent agreement with experimental observations. Substantial trapping in the physisorption well is observed after the impinging molecule loses its incidence energy to surface phonons and other molecular DOFs. Because of the large separation between the physisorbed molecule and the surface, EHPs play a minor role in vibrational relaxation. However, it is shown that facile energy loss in the vibrational DOF is enabled by the access to the chemisorption well. Hence, the experimentally observed CO(v=1) product is attributable to the fast nonadiabatic vibrational relaxation in the chemisorption well by EHPs, in which the rapid desorption of vibrationally relaxed CO constitutes the fast component of the experimental velocity distribution while the trapping in the physisorption well is responsible for the slow component. The dynamical simulations presented here offer an insightful understanding of some of striking experimental observations reported by Wodtke and coworkers.[22] These new insights have important implications in gas-metal interactions in general, particularly on the possible vibrational enhancement of reactivity for precursor-mediated surface reactions.

We acknowledge support by US National Science Foundation (CHE-1462109 to H.G.), National Key R&D Program of China (2017YFA0303500 to B.J.), National Natural Science Foundation of China (21573203, 91645202, and 21722306 to B.J.), Anhui Initiative in Quantum Information Technologies (AHY090200 to B.J.), and the Spanish Ministerio de Economía, Industria y Competitividad (FIS2016-76471-P to M.A.). H. G. also acknowledges Alec Wodtke, Dan Auerbach, Sascha Kandratsenka, and Igor Rahinov for several stimulating discussions and the Alexander von Humboldt Foundation for a Humboldt Research Award.

[1] J. C. Tully, Annu. Rev. Phys. Chem. **51**, 153 (2000).
[2] M. Alducin, R. Díez Muiño, and J. I. Juaristi, Prog. Surf. Sci. **92**, 317 (2017).
[3] S. P. Rittmeyer, V. J. Bukas, and K. Reuter, Adv. Phys. X **3**, 1381574 (2018).
[4] B. Jiang and H. Guo, J. Chem. Phys. **150**, 180901 (2019).
[5] R. Ryberg, Phys. Rev. B **32**, 2671 (1985).
[6] J. D. Beckerle, R. R. Cavanagh, M. P. Casassa, E. J. Heilweil, and J. C. Stephenson, J. Chem. Phys. **95**, 5403 (1991).
[7] M. Morin, N. J. Levinos, and A. L. Harris, J. Chem. Phys. **96**, 3950 (1992).
[8] T. A. Germer, J. C. Stephenson, E. J. Heilweil, and R. R. Cavanagh, J. Chem. Phys. **101**, 1704 (1994).
[9] B. N. J. Persson and M. Persson, Solid State Commun. **36**, 175 (1980).
[10] B. Hellsing and M. Persson, Phys. Scr. **29**, 360 (1984).
[11] T. T. Rantala and A. Rosén, Phys. Rev. B **34**, 837 (1986).
[12] M. Head-Gordon and J. C. Tully, J. Chem. Phys. **96**, 3939 (1992).
[13] V. Krishna and J. C. Tully, J. Chem. Phys. **125**, 054706 (2006).
[14] M. Forsblom and M. Persson, J. Chem. Phys. **127**, 154303 (2007).
[15] M. Askerka, R. J. Maurer, V. S. Batista, and J. C. Tully, Phys. Rev. Lett. **116**, 217601 (2016).
[16] R. J. Maurer, M. Askerka, V. S. Batista, and J. C. Tully, Phys. Rev. B **94**, 115432 (2016).
[17] D. Novko, M. Alducin, M. Blanco-Rey, and J. I. Juaristi, Phys. Rev. B **94**, 224306 (2016).
[18] R. Scholz, G. Floß, P. Saalfrank, G. Füchsel, I. Lončarić, and J. I. Juaristi, Phys. Rev. B **94**, 165447 (2016).
[19] S. P. Rittmeyer, J. Meyer, and K. Reuter, Phys. Rev. Lett. **119**, 176808 (2017).
[20] D. Novko, M. Alducin, and J. I. Juaristi, Phys. Rev. Lett. **120**, 156804 (2018).
[21] D. Novko, J. C. Tremblay, M. Alducin, and J. I. Juaristi, Phys. Rev. Lett. **122**, 016806 (2019).
[22] P. R. Shirhatti *et al.*, Nat. Chem. **10**, 592 (2018).
[23] D. P. Engelhart, R. J. V. Wagner, A. Meling, A. M. Wodtke, and T. Schäfer, Surf. Sci. **650**, 11 (2016).
[24] I. Lončarić, M. Alducin, J. I. Juaristi, and D. Novko, J. Phys. Chem. Lett. **10**, 1043 (2019).
[25] J. Wellendorff, K. T. Lundgaard, A. Møgelhøj, V. Petzold, D. D. Landis, J. K. Nørskov, T. Bligaard, and K. W. Jacobsen, Phys. Rev. B **85**, 235149 (2012).
[26] E. Dombrowski, E. Peterson, D. Del Sesto, and A. L. Utz, Catal. Today **244**, 10 (2015).
[27] S. Kumar, H. Jiang, M. Schwarzer, A. Kandratsenka, D. Schwarzer, and A. M. Wodtke, Phys. Rev. Lett. **123**, 156101 (2019).
[28] J. Behler and M. Parrinello, Phys. Rev. Lett. **98**, 146401 (2007).
[29] J. Behler, J. Chem. Phys. **134**, 074106 (2011).
[30] B. Kolb, X. Luo, X. Zhou, B. Jiang, and H. Guo, J. Phys. Chem. Lett. **8**, 666 (2017).
[31] Q. Liu, X. Zhou, L. Zhou, Y. Zhang, X. Luo, H. Guo, and B. Jiang, J. Phys. Chem. C **122**, 1761 (2018).
[32] K. Shakouri, J. Behler, J. Meyer, and G.-J. Kroes, J. Phys. Chem. Lett. **8**, 2131 (2017).
[33] Y. Zhang, X. Zhou, and B. Jiang, J. Phys. Chem. Lett. **10**, 1185 (2019).
[34] M. Head-Gordon and J. C. Tully, J. Chem. Phys. **103**, 10137 (1995).
[35] G. Kresse and J. Furthmuller, Phys. Rev. B **54**, 11169 (1996).
[36] G. Kresse and J. Furthmuller, Comp. Mater. Sci. **6**, 15 (1996).
[37] J. S. Smith, O. Isayev, and A. E. Roitberg, Chem. Sci. **8**, 3192 (2017).
[38] A brief discussion of the methods and numerical parameters used in our calculations, as well as additional results, can be found in Supplemental Material.
[39] Y.-l. Zhang, X.-y. Zhou, and B. Jiang, Chin. J. Chem. Phys. **30**, 727 (2017).
[40] X. Hu, W. L. Hase, and T. Pirraglia, J. Comput. Chem. **12**, 1014 (1991).
[41] M. C. Gutzwiller, *Chaos in Classical and Quantum Mechanics* (Springer, New York, 1990).
[42] Y. Li and G. Wahnström, Phys. Rev. Lett. **68**, 3444 (1992).
[43] P. M. Echenique, R. M. Nieminen, and R. H. Ritchie, Solid State Commun. **37**, 779 (1981).
[44] X. Luo, B. Jiang, J. I. Juaristi, M. Alducin, and H. Guo, J. Chem. Phys. **145**, 044704 (2016).
[45] J. I. Juaristi, M. Alducin, R. Díez Muiño, H. F. Busnengo, and A. Salin, Phys. Rev. Lett. **100**, 116102 (2008).
[46] D. Novko, M. Blanco-Rey, M. Alducin, and J. I. Juaristi, Phys. Rev. B **93**, 245435 (2016).
[47] M. J. Puska and R. M. Nieminen, Phys. Rev. B **27**, 6121 (1983).